International Conference on Renewable Energies and Power Quality (ICREPQ'18)
Salamanca (Spain), 21th to 23th March, 2018
Renewable Energy and Power Quality Journal (RE&PQJ)
ISSN 2172-038 X, No.16 March 2018

STUDY OF A FLAT PLATE SOLAR COLLECTOR WITH AN AIR CONDITIONER RADIATOR AS A HEAT ABSORBER FOR A DOMESTIC WATER HEATER

Vikas Reddy Chittireddy[1], Ahmed ElSawy[2*], and Stephen Idem[3]
[2] M.S. In Mechanical Engineering Candidate and [2, 3] Professors and Faculty Advisors
College of Engineering, Tennessee Technological University, Cookeville, Tennessee 38505, USA
Phone # 0019313723238/Fax # 0019313723813, emails: [1]vchittire42@students.tntech.edu,
[2*]aelsawy@tntech.edu, [3]Sidem@tntech.edu

Abstract. The objective of this study was to build a thermally efficient solar water heater. The receiver plate was constructed from an air conditioner radiator, and consisted of an array of serpentine tubes through which water was circulated. The presence of high density corrugated fins attached to the tubes increased the absorption of incident solar radiation. The flat plate collector was enclosed by double glazing which admitted solar radiation and minimized convection heat transfer losses to the environment. The shell of the collector was insulated to reduce conduction losses. A numerical model of flat plate solar collector thermal performance was developed and is likewise described in this paper. The model predicted the useful heat transfer to the water using an energy balance approach. An experimental program that was devised to verify the accuracy of the thermal performance model. Under certain circumstances close agreement was obtained between model predictions and experimental measurements, making the performance model of the flat plate solar collector a useful design tool.

Key words
Solar water heater, flat plate collector, double glazing, energy balance, Newton-Raphson method

1. Introduction

In the USA, water heaters may consume 15% to 25% of household energy every month. To reduce energy consumption for water heating, the use of solar water heaters is beneficial. A flat plate solar collector is a widely used solar water heater, and significant research is ongoing to improve efficiency. This paper describes a numerical model designed to predict solar water performance under a variety of environmental conditions, with a goal of using that model to suggest possible design improvements. The numerical model was evaluated with the help of experimental data.

Numerous experimental and modeling studies related to solar water heating systems have been reported in the literature; several of the more pertinent are herein discussed. Zelzouli et al. [1] concluded from his experiment that the number of collectors that can be connected in series is limited. When collectors are connected in series the outlet temperature of each collector will increase when compared to parallel or series-parallel connection, and this leads to an increase in thermal losses because of increased temperature differences. Jouhari et al. [2] demonstrated that by combining both flat plate and evacuated tube collectors the thermal performance of the compound collector was improved. Ben Slama [3] conducted experiments on an integrated flat plate/evacuated tubes collector, and found that the efficiency of double glazing was 42%, whereas by with single glazing the efficiency was 30%. Double glazing was more efficient because it reduced the night cooling effect. Experiments conducted by Ihaddadene et al. [4,5] demonstrated that increasing number of glazes reduced the performance of the solar collector. This was attributed to the high thermal resistance of the additional glass cover plates. It was also shown that as the distance between the two glass plates increased the performance decreased. Al-Khaffajy et al. [6] conducted solar water experiments using a single row heat exchanger and a double row heat exchanger with either elliptical or circular tubes. It was found that the temperature is higher in elliptical tubes than in circular tubes by 1ºC to 3ºC for same length and same cross section area. Shukla et al. [7] summarized the current state-of-the-art concerning system components of solar water heaters such as the collector, storage tank, and heat exchanger, and likewise discussed various approaches to improving performance and cost effectiveness of solar water heaters.

2. Numerical Model

The performance of a solar water heater is characterized by how efficiently it can convert the energy of incident solar energy to a corresponding increase in temperature of circulating hot water. The solar radiation incident on a horizontal surface consists of direct radiation E_D and diffuse radiation E_d. If the solar collector is facing due south into the sun and is oriented normally to the rays of the sun, the radiation incident on the collector equals the sum of the diffuse radiation and direct radiation

$$E_{collector} = E_D + E_d \quad (1)$$

In this study the diffuse radiation component was approximated per [8], and the direct radiation was measured. Natural convection heat transfer coefficient between the absorber plate and the lower cover plate, or between the lower and upper cover plates, was expressed in terms of an empirical Nusselt number for an inclined cavity. Since a

transition between the two types of fluid motion occurs at a critical tilt angle θ, with a corresponding change in the Nusselt number, Nu_L was calculated by the following formulas as a function of inclination angle

$$Nu_L = 1 + 1.44\left[1 - \frac{1708}{Ra_L\cos(\theta)}\right] \times \left[1 - \frac{1780(\sin(1.8\theta))^{1.6}}{Ra_L\cos(\theta)}\right] + \left[\left(\frac{Ra_L\cos(\theta)}{5830}\right)^{\frac{1}{3}} - 1\right] \quad (2)$$

Each term in brackets in Equation 2 was calculated as follows. If:

$$\left[1 - \frac{1780(\sin(1.8\theta))^{1.6}}{Ra_L\cos(\theta)}\right] < 0 \text{ then the value was 0}$$

$$\left[1 - \frac{1708}{Ra_L\cos(\theta)}\right] < 0 \text{ then the value was 0}$$

$$\left[\left(\frac{Ra_L\cos(\theta)}{5830}\right)^{\frac{1}{3}} - 1\right] < 0 \text{ then the value was 0}$$

In these expressions the quantity Ra_L is the Rayleigh number based on plate length L, and was given by

$$Ra_L = \frac{g\beta\Delta TL^3}{\nu^2}Pr \quad (3)$$

The quantity ΔT refers either to the temperature difference between the receiver and lower cover plate, or the lower and upper cover plates, depending upon the context. The variables β, ν, and Pr are thermal properties of air, which were evaluated at the film temperatures between the plates. The radiation heat transfer coefficient between the absorber plate and lower cover plate 1 was determined using

$$h_{r,pc1} = \frac{\sigma(T_p^2 + T_{c1}^2)(T_p + T_c)}{\frac{1}{\varepsilon_p} + \frac{1}{\varepsilon_g} - 1} \quad (4)$$

In this instance T_p is the absorber plate temperature, T_{c1} is the lower cover plate temperature, σ is Stefan-Boltzmann's constant (5.67×10^{-8} $Wm^{-2}K^{-4}$), and ε_p and ε_g are the absorber plate and cover plate emissivity, respectively. Likewise the radiation heat transfer coefficient between lower cover plate 1 and the upper cover plate 2 was evaluated as

$$h_{r,cc} = \frac{\sigma(T_{c1}^2 + T_{c2}^2)(T_{c1} + T_{c2})}{\frac{2}{\varepsilon_p} - 1} \quad (5)$$

In this case T_{c2} is the temperature of cover plate 2.

The thermal resistance concept was employed in this study to analyze heat transfer processes in the solar water heater. Therein the thermal resistance network is shown in Figure 1.

The equivalent thermal resistance for heat transfer between the absorber plate and cover plate 1 was expressed as

$$R_{eq1} = \frac{R_1^{"} \times R_2^{"}}{R_1^{"} + R_2^{"}} = \frac{\frac{1}{h_{r,pc}} \times \frac{1}{h_{pc}}}{\frac{1}{h_{r,pc}} + \frac{1}{h_{pc}}} \quad (6)$$

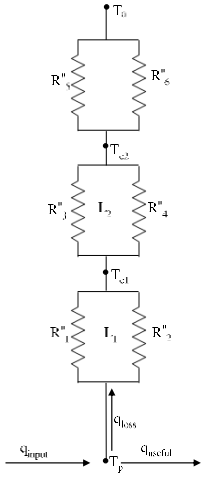

Fig. 1. Thermal resistance network

Likewise the equivalent thermal resistance for heat transfer between the lower cover plate and the upper cover plate was given by

$$R_{eq2} = \frac{R_3^{"} \times R_4^{"}}{R_3^{"} + R_4^{"}} = \frac{\frac{1}{h_{r,cc}} \times \frac{1}{h_{cc}}}{\frac{1}{h_{r,cc}} + \frac{1}{h_{cc}}} \quad (7)$$

Similarly the equivalent thermal resistance for heat transfer between the upper cover plate and the environment was expressed as

$$R_{eq2} = \frac{R_5^{"} \times R_6^{"}}{R_5^{"} + R_6^{"}} = \frac{\frac{1}{h_{r,ca}} \times \frac{1}{h_{ca}}}{\frac{1}{h_{r,ca}} + \frac{1}{h_{ca}}} \quad (8)$$

As these three resistance are in series, it implied

$$R_{eq} = R_{eq1} + R_{eq2} + R_{eq3} \quad (9)$$

Heat loss from the plate to the environment was given by

$$q_{loss}^{"} = \frac{T_p - T_a}{R_{eq}} \quad (10)$$

where T_a refers to the ambient air temperature. The fluid flowing through the absorber plate was water. In evaluating the thermal resistance terms the thermal properties for water were evaluated at the water inlet temperature, because the temperature rise through the solar collector was generally quite small for a given increment of time.

The water flow rate $\dot{m}$ and collector tube diameter D considered in this study implied that flow through the tubes was laminar. Therein the Seider-Tate correlation was used to evaluate the tube-side convection heat transfer coefficient

$$\overline{Nu_D} = 1.86(Re \times Pr)^{\frac{1}{3}}\left(\frac{D}{L_{Tube}}\right)^{\frac{1}{3}}\left(\frac{\mu}{\mu_s}\right)^{0.14} \quad (11)$$

where μ is viscosity of water. In this study the water outlet temperature T_o from the absorber was calculated assuming the tube wall temperature was constant and equal to the absorber plate temperature. A first law energy balance on the water tubes in the collector implied

$$T_0 = T_p - (T_p - T_i)\exp\left(-\frac{\bar{h}DL_{Tube}}{\dot{m}c_p}\right) \quad (12)$$

where T_i is the water inlet temperature. The heat transfer rate to the water by convection was

$$q = \dot{m}c_p(T_0 - T_i) \quad (13)$$

where c_p is the specific heat of water. Hence the useful heat flux to the water was given by

$$q''_{useful} = q/A \quad (14)$$

In this instance the quantity A denotes the projected surface area of the collector plate.

The Newton-Raphson method was used in this study to iteratively determine such parameters as the temperature of the receiver plate, cover plates 1 and 2, and the outlet water temperature. It is based on achieving an overall energy balance between the energy supplied by the sun versus the losses associated with radiation and convection to the environment, and the useful energy supplied to the water in the collector. Therein an energy balance on the receiver plate node yielded

$$f(T_p, T_{c1,} T_{c2}) = \tau^2\varepsilon_p E''_{collector} - q''_{useful} - q''_{loss} = 0 \quad (15)$$

An energy balance on the lower cover plate was expressed as

$$g(T_p, T_{c1,} T_{c2}) = (T_{c1} - T_{c2}) - q''_{loss}R_{eq\,1} = 0 \quad (16)$$

Similarly an energy balance on the upper cover plate was given by

$$h(T_p, T_{c1,} T_{c2}) = (T_{c2} - T_a) - q''_{loss}R_{eq\,2} = 0 \quad (17)$$

In this study two initial guesses were provided for the unknown nodal temperatures T_p, T_{c1}, and T_{c2}. Therein the partial derivatives of each function with respect to the unknown nodal temperatures were evaluated numerically. Subsequently these terms were substituted into the following 3 × 3 matrix equation

$$\begin{bmatrix} (\frac{\partial f}{\partial T_p})_{T_{c1},T_{c2}} & (\frac{\partial f}{\partial T_{c1}})_{T_p,T_{c2}} & (\frac{\partial f}{\partial T_{c2}})_{T_p,T_{c1}} \\ (\frac{\partial g}{\partial T_p})_{T_{c1},T_{c2}} & (\frac{\partial g}{\partial T_{c1}})_{T_p,T_{c2}} & (\frac{\partial g}{\partial T_{c2}})_{T_p,T_{c1}} \\ (\frac{\partial h}{\partial T_p})_{T_{c1},T_{c2}} & (\frac{\partial h}{\partial T_{c1}})_{T_p,T_{c2}} & (\frac{\partial h}{\partial T_{c2}})_{T_p,T_{c1}} \end{bmatrix} \begin{bmatrix} \Delta T_p \\ \Delta T_{c1} \\ \Delta T_{c2} \end{bmatrix} = \begin{bmatrix} -f_1 \\ -f_2 \\ -f_3 \end{bmatrix} \quad (18)$$

The solution of Equation 18 provided an iterative method for improving the approximate solution. The functions and the derivatives were evaluated using current values for the unknown nodal temperatures. Then an improved estimate of the solution was obtained using

$$T_p^{i+1} = T_p^i + \Delta T_p^i \quad (19)$$

$$T_{c1}^{i+1} = T_{c1}^i + \Delta T_{c1}^i \quad (20)$$

$$T_{c2}^{i+1} = T_{c2}^i + \Delta T_{c2}^i \quad (21)$$

The superscript i represents an iteration counter. The procedure continued until a prescribed convergence tolerance on the solution variables was achieved.

In the present study the water storage tank was thoroughly insulated to minimize heat losses. However, no attempt was made to measure standby losses. Therefore in this paper the following equation was employed to evaluate the thermal efficiency of the water heating system

$$\eta = \frac{\dot{m}c_p(T_0 - T_i)}{A \times E_{collector}}\,100 \quad (22)$$

3. Experimental Apparatus

Major components of the flat plate solar collector system considered in this paper were as follows: (i) the receiver plate (a repurposed air conditioner radiator), (ii) a water storage tank, (iii) the casing for the collector, as well as insulation on the bottom to reduce heat loss, (iv) two layers of glazing, (v) a linear actuator to control the inclination of the collector, and (vi) a water circulating pump. Other components included calibrated temperature sensors, a water mass flow rate sensor, and a data acquisition system. A three-row air conditioner radiator was selected as the receiver plate. Figure 2 shows the three-row design of an air conditioner radiator (without fins).

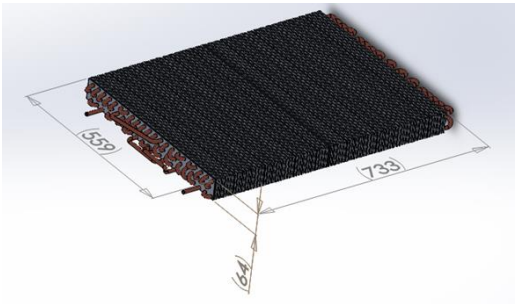

Fig. 2. Absorber plate (dimensions are mm)

The cross section area of the receiver plate was 0.73 m × 0.56 m. Each tube had an inner diameter of 7 mm and was 48 m long. There were a total number of 66 tubes in the radiator. The thickness of the fins was 0.25 mm, and there were 591 fins per meter. The material of the tubes was copper and the fins were constructed from aluminum. These fins were coated with black paint so as to increase solar absorptivity.

In the present experiment two acrylic sheets were employed as glazing for the solar collector. Plexiglas was used because it has a transmittance closely equivalent to optical glass. The total light transmittance of Plexiglas is 92% and the emissivity is 0.86 per [9]. In this experiment, double parallel glazing was used. Each glazing had a thickness of 6 mm. The distance between the two cover plates was 19 mm, and distance between the absorber plate and the lower cover plate was 36 mm. 11 type-T thermocouples were used to measure the temperature at prescribed locations on the receiver and cover plates, as well as the inlet and water temperatures. Three thermocouples were mounted to the upper cover plate, three were attached to the lower cover plate, and three thermocouples were affixed to the receiver plate, and the resulting values were averaged. Two thermocouples were used to measure the inlet and outlet temperatures of the receiver plate by inserting them directly into the 13 mm diameter steel pipes leading to/from the copper pipes in the radiator. Figure 3 shows the location of inlet and outlet thermocouples (1 and 2), and likewise illustrates the locations of the collector (2), flow sensor (3), storage tank (4), and circulation pump (5). Prior to installation in the solar water heater each temperature sensor was calibrated using a reference immersion thermometer. The water flow was measured using a calibrated flow sensor. The flow sensor required a voltage input of 5 to 18V DC (supplied by the data acquisition system). It was capable of measuring flow rates from 1 to 30 L/min over a temperature range of -25ºC to +80ºC. The water flow sensor was installed in a 1.5 m long pipe which was between the outlet of the collector and the storage tank. A sufficient length of pipe was employed upstream of the flow sensor to ensure the entering flow was fully-developed.

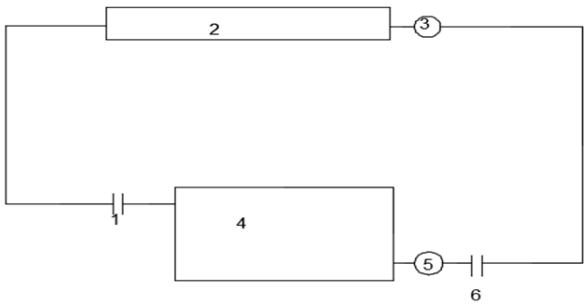

Fig. 3. Schematic diagram of test apparatus

The casing, receiver plate, and water storage tank were mounted on a moving trolley. The data acquisition system was placed on another moving trolley. Each time an experiment was performed the experimental setup mounted on the trolleys was moved out into an open area to receive solar radiation. In every instance the solar water heater was manually positioned facing towards the south during the acquisition of performance data. Once the setup was initially positioned the setup was not further adjusted, i.e., solar tracking was not employed while the measurements were performed. The casing was placed on horizontal bars which were capable of moving vertically. The horizontal bar was connected to a 12V DC linear actuator to raise the casing vertically in order to align the receiver place so that it was perpendicular to the solar irradiation at the start of the experiments. The storage tank was placed under the casing and a 12V DC circulating pump was connected to circulate the heat transfer fluid through the solar collector. The ambient temperature and solar insolation data were downloaded directly from a weather station located in the Tennessee Tech Millard Oakley STEM Center [10].

4. Results

The majority of testing was performed on clear sunny days in the summer of 2016. The measurements were carried out approximately five hours a day, and were initiated around noon when the sun was at the highest elevation. Data were acquired every 13 seconds, and the accompanying model calculations were performed on a 15-20 minute cycle. The goal of this aspect of the investigation was to demonstrate how closely the numerical predictions and the experimental data coincided. For brevity performance data only from July 20, 2016 are presented herein. Table 1 displays the input values to the model that were either measured or inferred, and which were assumed to be constant in the subsequent analysis. Because the external heat transfer coefficient associated with the upper cover plate was not measured and was subject to significant uncertainty, a value for the heat transfer coefficient of h_{ca} = 9 W/m^2·˚C was assumed for these baseline cases. However, the model also employed solar irradiation and ambient temperature data taken from the TTU STEM Center as input, and these values were assumed to vary with time. Likewise the time-varying water temperature measured in the pipe situated between the insulated storage and the receiver was treated as a transient input to the numerical model. In each instance these values were updated on a 13 second interval.

Table 1. Input values employed in numerical model

ε_p	ε_c	τ
0.86	**0.86**	**0.92**
D (mm)	**L_{tube} (m)**	**$H_{absorber}$ (m)**
7	**48.6**	**0.06**
L_1 (m)	**L_2 (m)**	**$A_{absorber}$ (m^2)**
38	**19**	**0.41**
Θ (deg)	**h_{ca} (W/m^2-˚C)**	**$\dot{m}$ (kg/s)**
8	**9**	**0.029**

For the test performed on July 20, 2016, the measured water outlet temperature is compared to the predicted outlet water and plotted as a function of time in Figure 4. Transient values

of the measured solar water heater thermal efficiency calculated using Equation 22 are also shown in Figure 4. The corresponding instantaneous values of solar irradiation and ambient temperature are illustrated in Figure 5. During the test the water outlet temperature rose continuously as a function of time. The thermal efficiency of the solar water heater ranged between 60% to 90%. In this instance the thermal efficiency increased initially until approximately noon time, and thereafter was constant.

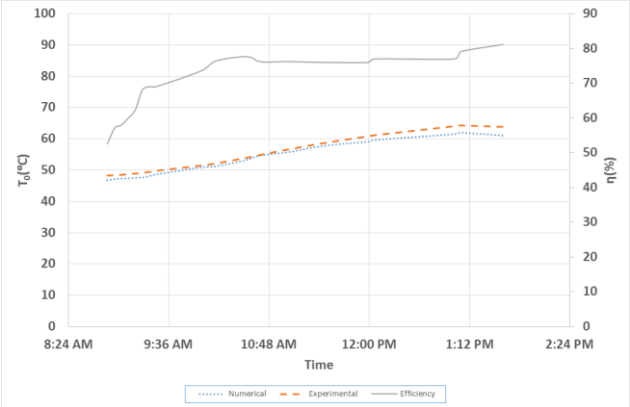

Fig. 4. Numerical analysis, experimental data, and efficiency vs. time on July 20

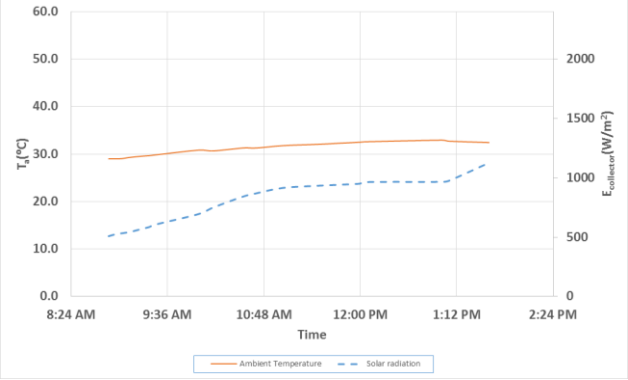

Fig. 5. Ambient temperature and solar radiation vs time on July 20

The numerical solar water heater thermal model generally under-predicted important performance parameters such as measured water outlet or receiver plate temperature. Information on several important inputs to the numerical model described previously were either lacking or subject to a degree of uncertainty. Therefore a detailed parametric study was performed on model input variables such as absorber plate emissivity, cover plate emissivity, cover plate transmissivity, the gap between the upper cover plate and lower cover plate or between the lower cover plate and the receiver plate, water mass flow rate, and solar insolation. The intention was to examine a range over which a variable may exist, in order to investigate how this uncertainty affects the results of the model. These investigations demonstrated that uncertainties in the absorber and/or cover plate radiation properties had limited impact on the predictive capability of the numerical model. An additional parametric study was performed wherein the external heat transfer coefficient h_{ca} was likewise varied over a range from 9 W/m^2·˚C to 19 W/m^2·˚C, in order to assess the impact of that value on model predictions of water outlet and receiver plate temperatures., but it was determined that varying the heat transfer coefficient over the prescribed range was incapable of accounting for the observed differences. For brevity the results of those investigation are not included herein.

Uncertainties associated with the water flow rate could have a significant impact on water outlet temperature and receiver plate temperature. Figure 6 displays the effects on water outlet temperature when the water mass flow rate was systematically varied over a range of 0.025 kg/sec to 0.033 kg/sec. These values constitute ±15% of the actual measured ṁ = 0.029 kg/sec that was used to generate the results presented in Figure 4. Reducing the water mass flow rate improved model predictions of outlet water temperature, but the assumed uncertainty in the water mass flow rate did fully account for the noted discrepancies between measured and predicted values of the water outlet and receiver temperature. However, Figure 6 clearly implies that reducing the mass flow rate had the effect of increasing the water outlet temperature.

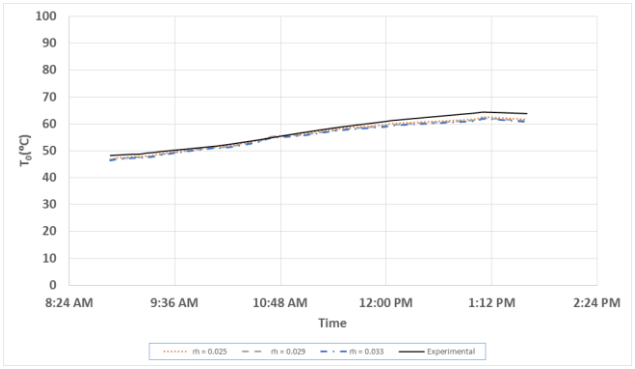

Fig. 6. Parametric study on water outlet temperature with water mass flow rate ṁ = 0.019 kg/sec, 0.029 kg/sec, and 0.033 kg/sec

A parametric study was performed to study the impact of measured solar insolation uncertainty on water outlet temperature. In this instance an uncertainty of ±15% on the values of $E_{collector}$, as determined using Equation 6 and based on solar radiation data taken from TTU STEM Center. Therein Figure 7 displays the effects on the water outlet and receiver plate temperature by varying the range of calculated $E_{collector}$ by ±15%, relative to the measured amount. It is apparent that increasing $E_{collector}$ by 15% yielded calculated water outlet temperatures that closely matched measured temperatures.

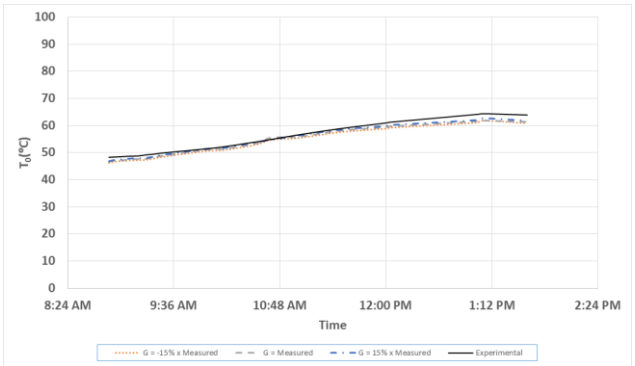

Fig. 7. Parametric study on water outlet temperature with ±15% change in solar radiation

5. Conclusions

This paper has described the thermal performance of a double-glazed solar water heater that incorporated an air-conditioning radiator as the collector. Kalidasan et al. [11] demonstrated that the efficiency of a flat plate solar water heater was a function of the number of cover plates. In experiments conducted with one cover plate the instantaneous efficiency was 51.5%, whereas with two cover plates the efficiency was 61.7%, and with three cover plates the efficiency was 56.5%. By comparison, overall thermal efficiencies of the solar water heater design considered in the present study ranged from 60% to 90%. A numerical model of flat plate solar collector thermal performance was developed and is also described in this paper. The model predicted the useful heat transfer to the water using an energy balance approach. The Newton-Raphson method was used to iteratively solve for the unknown receiver and cover plate temperatures. The analysis fully accounted for natural convection and radiation exchange between the receiver and cover plates, as well as heat losses to the environment. An experimental program was devised to verify the accuracy of the thermal performance model. The solar water heater was fully instrumented to measure such variables as water flow rate and temperature rise, solar insolation, and receiver and cover plate temperatures. The numerical solar water heater thermal model generally under-predicted such important performance parameters as the measured water outlet or receiver plate temperatures.

A parametric study was performed to investigate the effects of uncertainties associated with key individual thermal model input data on predicted solar water heater performance. Simultaneous variation of all inputs to the model was prohibitive, due to the large number of variables. The parametric study revealed that uncertainties in the absorber plate emissivity, cover plate emissivity, and the cover plate transmissivity did not have a significant effect regarding model predictions of water outlet temperature and receiver plate temperature. Likewise when the distance between the cover plates was reduced the predicted water outlet temperature and receiver plate temperature exhibited a modest increase. However it was observed that reducing the water mass flow rate or increasing the solar insolation input values to the model over a reasonable range of uncertainty yielded relatively close agreement between measured and predicted outlet water outer temperature. This implies that future experimental efforts should concentrate on measuring those particular quantities with particular care.

In this study it was assumed that all heat transfer processes were steady in nature. For example, the model was incapable of fully accounting for gradual variations in direct solar insolation associated with the progression of the sun across the sky, or for relatively rapid changes in solar insolation due to changes in cloud cover. The likely presence of a temperature drop across the thickness of each cover plate (because of conduction effects) was not accounted for in the model. The thermal model of the solar water heater likewise employed a gray surface radiation model for the cover and receiver plates. In many instances glass cover plates are relatively opaque to longer wavelength infrared radiation, i.e., they tend to retain much of the shorter wavelength solar radiation incident upon the plate surface. That effect was not accounted for in the performance model. Despite these modest deficiencies, it is concluded that relatively close agreement was obtained between model predictions and experimental measurements, thus making the performance model of the flat plate solar collector a useful design tool. Further versions of the solar water heater apparatus should incorporate cover plate materials which enhance retention of incident solar radiation by proper control of longer wavelength infrared radiation. The proposed solar water heater design can be improved by adding a solar tracker to help synchronize the receiver orientation with the location of the sun.

6. References

1. Zelzouli, K., Guizani, A., Sebai, R. and Kerkeni, C. (2012), "Solar Thermal Systems Performances versus Flat Plate Solar Collectors Connected in Series," Engineering, Vol. 4, No. 12, pp. 881-893. doi: 10.4236/eng.2012.412112.
2. Jouhari, M., Touhmeh, S. and Moukhayber, N. (2015), Manufacturing and Thermal Performance Test of (Compound) Solar Collector in Damascus City. Journal of Biomedical Science and Engineering, Vol. 8, pp. 370-379. doi:10.4236/jbise.2015.86035.
3. Ben Slama, R. (2012), "Experimentation of a Plane Solar Integrated Collector Storage Water Heater," Energy and Power Engineering, Vol. 4, No. 2, pp. 67-76. doi: 10.4236/epe.2012.42010.
4. Ihaddadene, N., Ihaddadene, R., Mahdi, A. (2014), "Effect of Glazing Number on the Performance of a Solar Thermal Collector", International Journal of Science and Research, Vol. 3, Issue 6, pp. 1199-1203.
5. Ihaddadene, N., Ihaddadene, R., Mahdi, A. (2014), "Effect of Distance between Double Glazing on the Performance of a Solar Thermal Collector", International Conference on Renewable Energies and Power Quality (ICREPQ'14) Cordoba (Spain), pp. 302-306.
6. Al-Khaffajy, M. and Mossad, R. (2013), "Optimization of the Heat Exchanger in a Flat Plate Indirect Heating Integrated Collector Storage Solar Water Heating System", Renewable Energy, volume 57, pp. 413-421.
7. Shukla, R., Sumathy, K., Erickson, P., and Gong, J. (2013), "Recent advances in the solar water heating systems: A review," Renewable and Sustainable Energy Reviews, Vol. 19, pp. 173-190.
8. ASHRAE. 2013. ASHRAE Handbook – Fundamentals, Chapter 4, Atlanta: American Society of Heating, Refrigerating and Air-Conditioning Engineers, Inc.
9. http://www.plexiglas.com/export/sites/plexiglas/.content/medias/downloads/sheet-docs/plexiglas-general-information-and-physical-properties.pdf.
10. https://www.wunderground.com/personal-weather-station/dashboard?ID=KTNCOOKE16#history.
11. Kalidasan, B. and Srinivas, T. (2014), "Study on Effect of Number of Transparent Covers and Refractive Index on Performance of Solar Water Heater," Journal of Renewable Energy, Article ID 757618. doi:10.1155/2014/757618.